32nd Annual International Conference of the IEEE EMBS
Buenos Aires, Argentina, August 31 - September 4, 2010

A 64-Channel Readout ASIC for Nanowire Biosensor Array with Electrical Calibration Scheme

Kevin T. C. Chai, *Member, IEEE*, Kunil Choe, Olivier D. Bernal, *Member, IEEE*, Pradeep K. Gopalakrishnan, *Senior Member, IEEE*, Guo-Jun Zhang, Tae Goo Kang, Minkyu Je, *Member, IEEE*

***Abstract*— A 1.8-mW, 18.5-mm^2 64-channel current readout ASIC was implemented in 0.18-μm CMOS together with a new calibration scheme for silicon nanowire biosensor arrays. The ASIC consists of 64 channels of dedicated readout and conditioning circuits which incorporate correlated double sampling scheme to reduce the effect of 1/f noise and offset from the analog front-end. The ASIC provides a 10-bit digital output with a sampling rate of 300 S/s whilst achieving a minimum resolution of 7 pA$_{rms}$. A new electrical calibration method was introduced to mitigate the issue of large variations in the nano-scale sensor device parameters and optimize the sensor sensitivity. The experimental results show that the proposed calibration technique improved the sensitivity by 2 to 10 times and reduced the variation between dataset by 9 times.**

I. Introduction

BIOSENSOR arrays have become important tools for highly parallel bioanalysis, and fully electronic biosensor arrays have been recently reported [1-3]. They can avoid expensive and bulky optical equipment and some [1], [2] even exclude costly labeling process. These properties open the door to point-of-care diagnosis. However, most electronic biosensor arrays are based on a combination of simple microelectrode arrays, electrochemical reactions, and electronic sensing circuits [1-3], which have sensitivities inferior to the optical detection method [4].

In recent years, silicon nanowires (SiNWs) have widely been investigated as ultra-sensitive biosensors and chemical sensors for ions, DNA [5], proteins [6], virus and cells. Benefiting from a large surface-to-volume ratio, the SiNW sensor achieves ultra-high sensitivity. Typically a few nA current flows through SiNWs and a few hundreds of pA change occurs when pM level of target DNA sequences are hybridized [5] or pg/ml level of target proteins are bound [6] on its surface. It implies that comparable or even better sensitivity than optical methods can be achieved so that the point-of-care diagnosis based on fully electronic biosensor arrays can be realized. However, the sensor sensitivity is strongly affected by the variation in the electrical properties of the nano-scale devices [7].

This work presents a 64-channel readout ASIC for SiNW biosensor array and introduces a new electrical calibration method to address the problems caused by the variations in the electrical properties of SiNWs.

Manuscript received April 1, 2010.

K. T. C. Chai and M. Je are with the Integrated Circuits and Systems Laboratory, Institute of Microelectronics, A*STAR (Agency of Science, Technology and Research), Singapore (Phone: +65-6770-5548; fax: +65-6778-0136; e-mail: chaitc@ime.a-star. edu.sg).

G-J. Zhang and T. G. Kang are with the Bioelectroincs Programme, Institute of Microelectronics, A*STAR (Agency of Science, Technology and Research), Singapore.

O. D. Bernal was with the Integrated Circuits and Systems Laboratory, Institute of Microelectronics, A*STAR (Agency of Science, Technology and Research), Singapore. He is now with the Department of Electronics, University of Toulouse INP-LOSE, France.

K. Choe was with the Integrated Circuits and Systems Laboratory, Institute of Microelectronics, A*STAR (Agency of Science, Technology and Research), Singapore. He is now with the Electrical Engineering Department, Yale University, Connecticut, USA.

P. K. Gopalakrishnan was with the Integrated Circuits and Systems Laboratory, Institute of Microelectronics, A*STAR (Agency of Science, Technology and Research), Singapore. He is now with RV-VLSI Design Center, Bangalore, India.

II. Field-Effect-Based Biosensing and Electrical Calibration Method

A. Field-Effect-Based SiNW Biosensors

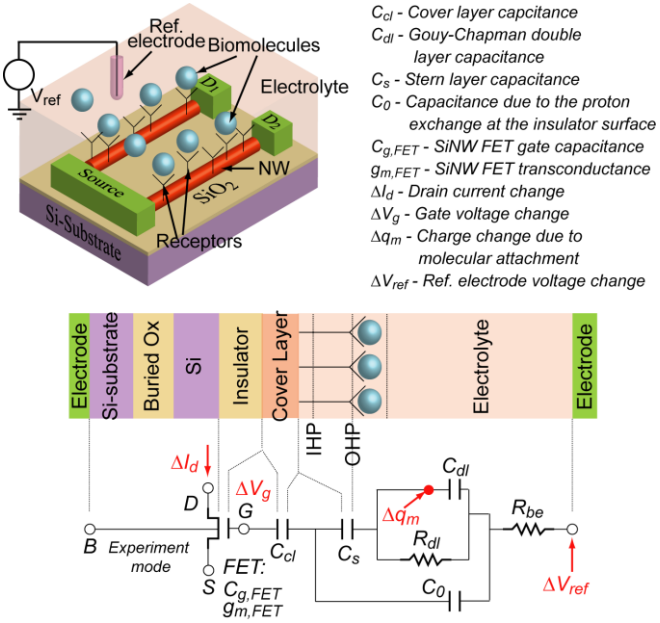

Fig. 1. Conceptual diagram of SiNW biosensor operation and its equivalent circuit model [8]. The equivalent circuit model is modified from the electrical double layer model for the SiO_2 dielectric surface. The modification is completed by the addition of the cover layer (C_{cl}) to account for the extra functionalized layer (receptors).

The operation principle of SiNW biosensors is shown in Fig. 1. The SiNW FET does not have a physical gate, and hence it requires a reference electrode to establish its gate potential through the electrolyte. The surface of the gate

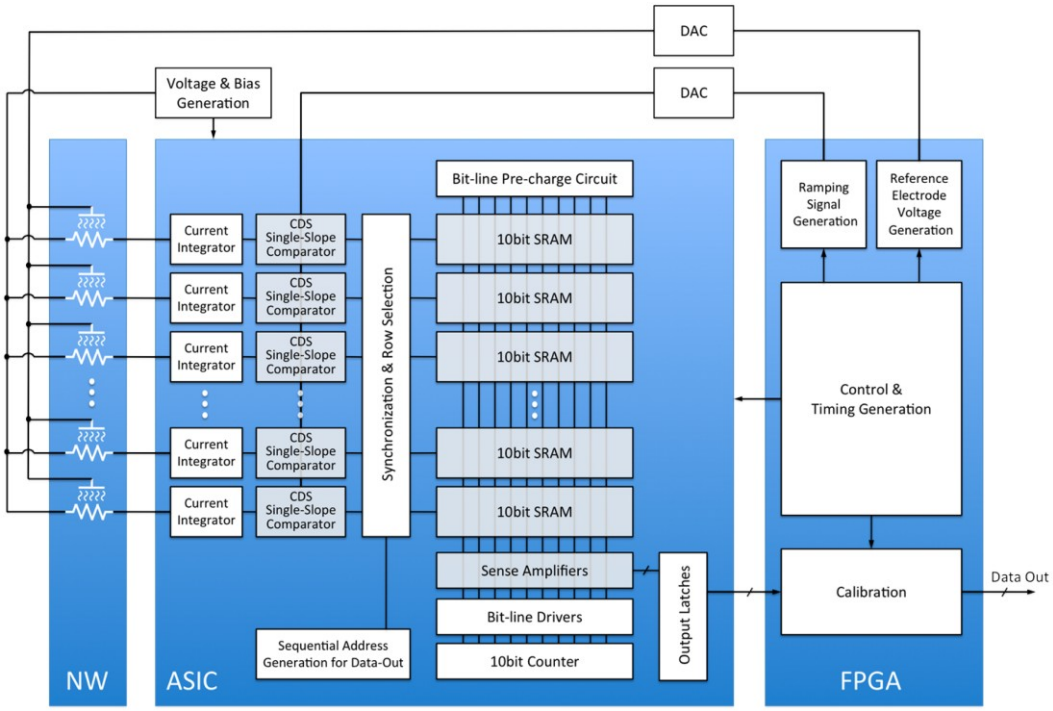

Fig. 2. Block diagram of SiNW biosensor measurement system consisting of a SiNW biosensor array, a dedicated 64-channel readout ASIC and an FPGA.

insulation is functionalized with a layer of probe molecules (receptors) that is specific to the targeted biomolecules.

On successful binding, the effective electric charge of the targeted biomolecules creates a localized potential gradient which results in a threshold voltage shift in the SiNW biosensor. The equivalent circuit model of the general field-effect biosensors [8] is also shown in Fig. 1. The circuit model includes the description of the electrical double layer and an additional cover layer functionalized with probe molecules.

B. Calibration Algorithm

$$S_{qm} \equiv \frac{\Delta I_d / I_d}{\Delta q_m} = \frac{\Delta g_{m,FET}}{\Delta q_m} \times \frac{g_{m,FET}}{I_d} \tag{1}$$

$$S_{cal} \equiv \frac{\Delta I_d / I_d}{\Delta V_{ref}} = \frac{\Delta g_{m,FET}}{\Delta V_{ref}} \times \frac{g_{m,FET}}{I_d} = \frac{\Delta I_d / \Delta V_{ref}}{I_d} = \frac{g_{m,eff}}{I_d} \tag{2}$$

$$S_{qm} \equiv \frac{C_{dl}C_s + C_{dl}C_0 + C_sC_0}{C_s} \times S_{qm} \tag{3}$$

The SiNW biosensor sensitivity S_{qm} in (1) is defined by the change in drain current $\Delta I_d / I_d$ as a result of the effective charge change Δq_m caused by molecular binding. S_{qm} can vary significantly because it is affected by the surface chemistry, device parameters such as trapped oxide charges, gate oxide thickness, channel dimensions and doping concentration of the SiNW. This work proposes to use a small-signal change in the reference electrode voltage instead of the real molecular charge attachment to estimate S_{qm}. Then, the calibration factor S_{cal} in (2) is obtained from the measurement of the effective transconductance $g_{m,eff}$ ($\equiv \Delta I_d / \Delta V_{ref}$) and I_d. From (3), S_{cal} is directly proportional to S_{qm} with the proportionality factor of $(C_{dl}C_s + C_{dl}C_0 + C_sC_0) / C_s$. All capacitors in this factor are very weak functions of V_{ref} compared to $C_{g,FET}$ and $g_{m,FET}$ [9], and hence the factor can be regarded as a constant. Therefore, S_{cal} is a good measure of S_{qm}, and can be used for the calibration.

The calibration procedure is as follows: for an array of SiNW biosensors, (a) I_d is measured over a range of V_{ref}; (b) $g_{m,eff}$ is calculated as a function of V_{ref}; and (c) S_{cal} is calculated and used for normalization of the results between sensors. This technique can also be used to optimize the sensors' sensitivity. The value of S_{cal} increases as V_{ref} decreases and peaks in the subthreshold region, hence operating in the subthreshold region can maximize the sensitivity.

III. Circuit Design and System Architecture

Fig. 2 shows the block diagram of the measurement system consisting of a SiNW biosensor array, a 64-channel readout ASIC and an FPGA. The FPGA generates control signals and ramp signal for the ASIC, sweeps reference electrode voltage, and executes the calibration algorithm on the measured data. The circuit diagram of each readout channel is shown in Fig. 3.

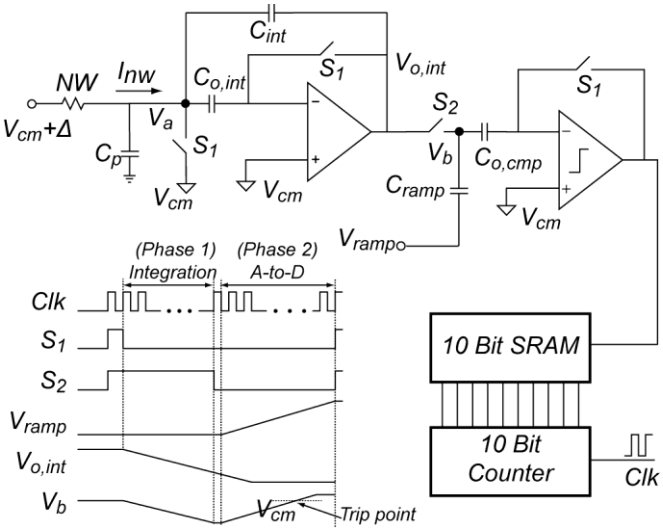

Fig. 3. Circuit diagram and control timing diagram of a single-channel readout circuit.

Each readout channel is dedicated to a single SiNW and it consists of a charge integrator, a comparator and a 10-bit SRAM. The charge integrator and the comparator form the analog front-end and they are configured to implement a correlated double sampling (CDS) scheme which helps to reduce the offset and 1/f noise. The bus of the 10-bit SRAM is connected to a global counter through bit-line drivers (Fig. 2), and together with the charge integrator and the comparator forms a CDS single-slope ADC to provide a digital readout.

Phase 1 operation starts with the offset cancellation process. When S_1 closes, the offset voltages of the charge integrator and the comparator are stored on capacitors $C_{o,int}$ and $C_{o,cmp}$ respectively. Subsequently, when S_1 opens, the offset is cancelled. Similarly, C_{ramp} is used to cancel the offset from the ramp signal. After offset cancellation, I_{nw} is integrated across C_{int}. Note that the integration time can be adjusted to fit different input current ranges. S_2 is closed during phase 1 and opened in phase 2. The rising ramp signal V_{ramp} is applied to V_b during the A/D conversion in Phase 2. At the same time, the global counter is initiated. V_{ramp} signal toggles the comparator output when the total summed voltage across $C_{o,cmp}$ becomes greater than V_{cm}. Consequently, the trip signal from the comparator causes the SRAM to capture the counter value, and the contents in the SRAM becomes the digital presentation of the input current I_{nw}.

IV. Results and Discussion

Fig. 4 shows the results recorded with the ASIC from a controlled current source. The results were obtained by sweeping the input current from 100 pA to 8 nA for an integration time of 3 ms. V_{out} is the converted digital output with respect to the different values of I_{nw}.

The results show a linear output response up to 5.3 nA, which is sufficient for typical SiNW biosensor measurements. However, dynamic range can be further improved by adjusting the integration time. The inset of Fig. 4 shows the time-domain fluctuation of the measured current when the mean current is 2.31 nA. The equivalent noise of 7 pA_{rms} at 300 Hz bandwidth is observed and the leakage current was 680 fA, indicating that the ASIC can measure input current changes in the sub-100-pA range with sufficient signal-to-noise ratio.

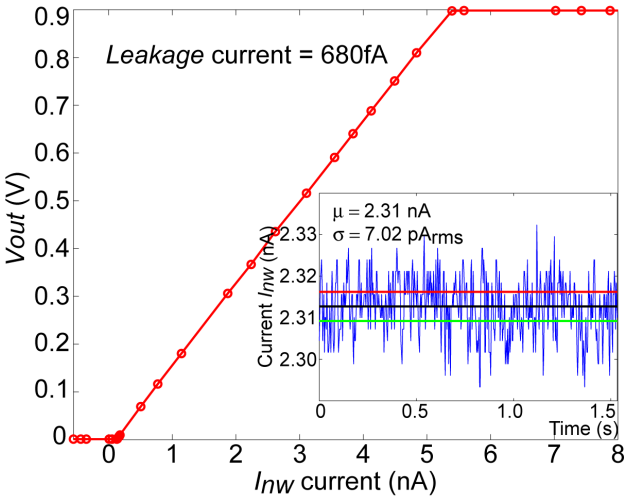

Fig. 4. Electrical measurement result of the readout ASIC showing the input current I_{NW} vs. output voltage response V_{out} and the noise performance. The input current noise measurement achieved a minimum resolution of 7 pA_{rms} when measured with a nominal input current value of 2.31 nA.

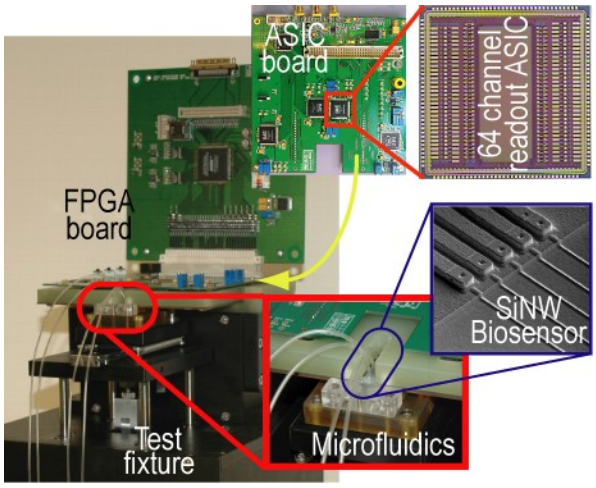

Fig. 5. Overall set-up of the 256-channel readout system consisting of a test fixture that holds a biosensor chip including 256 SiNWs, microfluidics, an ASIC board with four 64-channel ASICs and an FPGA board.

Fig. 5 shows the overall set-up of the 256-channel readout system using a biosensor chip including 256 SiNWs interfaced with four 64-channel ASICs and an FPGA board. The test fixture uses microprobes to establish the electrical connections between the biosensor chip and the ASIC board.

The ASIC chip was fabricated in 0.18-μm CMOS technology with metal-insulator-metal (MIM) capacitor option (Fig. 6). Approximately 120,000 transistors were integrated in die area of 4.3 mm × 4.3 mm. The chip consumes only 1 mA from 1.8-V supply for 64-channel readout, which is suitable for point-of-care diagnosis and implies its scalability to larger size of biosensor arrays.

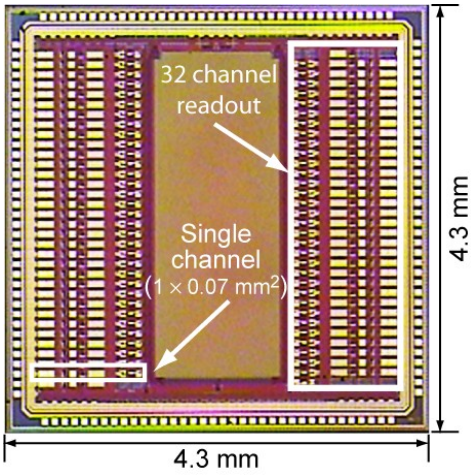

Fig. 6. Chip micrograph (technology: 0.18-μm CMOS with MIM capacitor option).

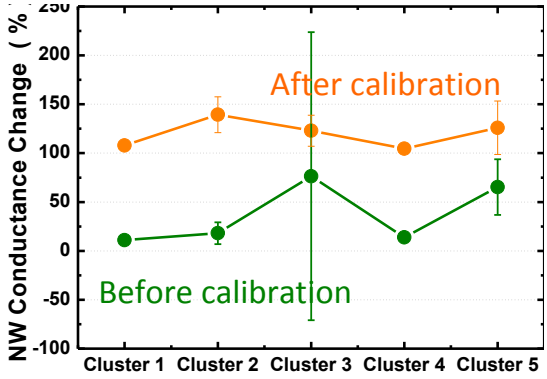

Cluster	Conductance Change without Calibration			Conductance Change with Calibration		
	Mean	Std. dev.	CV	Mean	Std. dev.	CV
1	10.97	0.88	0.08	107.92	4.27	0.04
2	18.14	11.19	0.62	139.36	18.36	0.13
3	76.40	147.4	1.93	122.98	15.90	0.13
4	13.82	3.62	0.26	104.51	4.38	0.04
5	65.32	28.44	0.44	125.98	27.27	0.22

Fig. 7. Statistical data of the measurement from 1-ng/ml cTnT detection using the SiNW biosensor array.

The SiNWs were prepared for the detection of troponin-T (cTnT), which is a key protein biomarker for cardiovascular diseases. The preparation procedure can be found in [6]. Fig. 7 shows the results of 1-ng/ml cTnT binding on the SiNWs. The results were obtained from 5 clusters, each with 20 SiNWs. Before calibration, the conductance change showed mean values ranging from 11% to 76% and the largest coefficient of variation (CV) value of 1.9. When the calibration was applied, the mean values range from 104% to 139% and the largest CV value of only 0.22 were observed. It shows that the calibration method significantly improves not only the statistics but also the sensitivity of SiNW biosensors. The improvement in the mean values from the calibrated data was attributed to the optimal selection of biasing points that set the SiNWs in their subthreshold region.

V. Conclusion

We have presented our work on a 64-channel, 10-bit digital output readout ASIC for SiNW biosensor array. The readout circuit for each channel is a CDS single-slope ADC consisting of a charge integrator, a comparator and a 10-bit SRAM. Electrical measurement from each channel showed leakage current of 680 fA and noise resolution of 7 pA_{rms}, making it suitable for the detection of sub-100-pA detection from pg/ml concentration of protein molecules using the SiNW biosensor array. The electrical calibration algorithm was able to improve on the sensitivity measurement by 2 to 10 times and reduce the variation in the datasets by 9 times.

Acknowledgment

The author would like to thank H. Z. H. Luo, M. J. Huang and I. G. K. Tay for their technical support and F. Cheng for his helpful discussion on the use of reference electrode.

References

[1] F. Heer, M. Keller, G. Yu, J. Janata, M. Josowicz, A. Hierlemann, "CMOS electro-chemical DNA-detection array with on-chip ADC," *ISSCC Dig. Tech. Papers*, pp. 168-169, Feb. 2008.

[2] N. Gemma, S. O'uchi, H. Funaki, J. Okada and S. Hongo, "CMOS integrated DNA chip for quantitative DNA analysis," *ISSCC Dig. Tech. Papers*, pp. 560-561, Feb. 2006.

[3] M. Augustyniak, C. Paulus, R. Brederlow, N. Persike, G. Hartwich, D. Schmitt-Landsiedel, R. Thewes, "A 24×16 CMOS-based chronocoulometric DNA microarray," *ISSCC Dig. Tech. Papers*, pp. 46-47, Feb. 2006.

[4] B. Jang, P. Cao, A. Chevalier, A. Ellington, A. Hassibi, "A CMOS fluorescent-based biosensor microarray," *ISSCC Dig. Tech. Papers*, pp. 436-437, Feb. 2009.

[5] G-J. Zhang, G. Zhang, J. H. Chua, R-E. Chee, E. H. Wong, A. Agarwal, K. D. Buddharaju, N. Singh, Z. Gao, N. Balasubramanian, "DNA sensing by silicon nanowire: charge layer distance depencence," *Nano Lett.*, vol. 8, pp. 1066-1070, Apr. 2008.

[6] J. H. Chua, R-E. Chee, A. Agarwal, S. M. Wong, G-J Zhang, "Label-free electrical detection of cardiac biomarker with complementary metal-oxide-semiconductor-compatible silicon nanowire sensor arrays," *Anal. Chem.*, vol. 81, pp. 6266-6271, Aug. 2009.

[7] M. Abe, K. Murata, T. Ataka, K. Matsumoto, "Calibration method for a carbon nanotube field-effect transistor biosensor," *Nanotechnology*, vol. 19, p. 045505, Jan. 2008.

[8] M. W. Shinwari, M. J. Deen, P. Selvaganapathy, "Analytic modeling of biotransistors," *IET Circuits Devices Syst.,* vol. 2, pp. 158-165, Feb. 2008.

[9] D. Landheer, G. Aers, W. R. McKinnon, M. J. Deen, J. C. Ranuarez, "Model for the field effect from layers of biological macromolecules on the gates of metal-oxide-semiconductor transistors," *J. Appl. Physics,* vol. 98, p. 044701, Aug. 2005.